



# Hydrocarbon superhydrophobic polymers from electrochemical polymerization: an alternative to fluorine?

Mélanie Wolfs

## ► To cite this version:

Mélanie Wolfs. Hydrocarbon superhydrophobic polymers from electrochemical polymerization: an alternative to fluorine?. Material chemistry. Université Nice Sophia Antipolis, 2013. English. NNT : . tel-00933342

**HAL Id: tel-00933342**

**<https://theses.hal.science/tel-00933342>**

Submitted on 20 Jan 2014

**HAL** is a multi-disciplinary open access archive for the deposit and dissemination of scientific research documents, whether they are published or not. The documents may come from teaching and research institutions in France or abroad, or from public or private research centers.

L'archive ouverte pluridisciplinaire **HAL**, est destinée au dépôt et à la diffusion de documents scientifiques de niveau recherche, publiés ou non, émanant des établissements d'enseignement et de recherche français ou étrangers, des laboratoires publics ou privés.

UNIVERSITE DE NICE-SOPHIA ANTIPOLIS - UFR Sciences  
Ecole Doctorale « Sciences Fondamentales et Appliquées »

## THÈSE

pour obtenir le titre de

Docteur en Sciences  
de l'UNIVERSITE de Nice-Sophia Antipolis

Discipline : Chimie

Présentée et soutenue par

**Mélanie WOLFS**

### **HYDROCARBON SUPERHYDROPHOBIC POLYMERS FROM ELECTROCHEMICAL POLYMERIZATION: AN ALTERNATIVE TO FLUORINE?**

Thèse dirigée par le Professeur Frédéric GUITTARD et le Docteur Thierry DARMANIN

Soutenue le 13 / 12 / 2013 devant le Jury composé de

|             |  |                       |
|-------------|--|-----------------------|
| E. Magnier  | Directeur de Recherches au CNRS, Institut Lavoisier de Versailles,<br>Université de Versailles-Saint-Quentin, France | Rapporteur            |
| V. Ravaine  | Maître de Conférences - HDR, Institut des Sciences Moléculaires,<br>Université Bordeaux 1, France                    | Rapporteur            |
| F. Guittard | Professeur, Université de Nice-Sophia Antipolis, France  | Directeur de thèse    |
| T. Darmanin | Maître de Conférences, Université de Nice-Sophia Antipolis,<br>France  | Co-directeur de thèse |
| S. Pommeret | HDR, Président de la division Chimie-Physique de la Société<br>Chimique de France, France                            | Examineur             |
| R. Ras      | Professeur , Department of Applied Physics, Aalto University,<br>Finland   | Examineur             |

# Acknowledgments

First of all, I would like to thank Professor Frédéric Guittard for allowing me to do this PhD thesis in his research group, for his fruitful discussions about the research project but also about the doctor position. I also thank him for let me the opportunity to represent the laboratory all over the world. It was a real honor.

My thanks also go to Doctor Thierry Darmanin, co-director of this work for his involvement, his availability and his constructive discussions to move research forward together.

I would like to thank Doctor Valérie Ravaine and Doctor Emmanuel Magnier for being reviewers of this work. I also thank Doctor Stanislas Pommeret as well as Professor Robin Ras for their participation in the jury as examiners.

My thanks then go to the permanent staff of the research group: Sonia, Elisabeth but also Catherine, who was an invaluable help in the research group administration.

I sincerely thank all the members of the research group: Elena, Arnaud, Jeanne, Sabri, Cécile, Janwa, Olivier but also Abdoulaye, Chahinez, Alioune. I do not forget the past members Doctor Carine, Doctor Mamadou, Doctor Gennifer, Doctor Hervé I worked with. It was a great pleasure to work in such a good atmosphere and to share discussions, cakes, lunches and other great moments.

I would like to thank Jean-Pierre Laugier for the precious SEM images otherwise this work had not been so beautiful. It was each time a great pleasure to receive these images, synonymous of great surprises with new morphologies.

My thanks also go to the trainees I had the opportunity to supervise during these three years: Adil Jabbari, Marion Raffaldi, Florence Uvernet and Nicolas Vigneau.

Then I would like to thank Salomé and all the people I have met during my studies in Bordeaux: Morgane G., Guillaume, JP, Morgane L., Camille, Clémence, Maxime, Laura, Marie-Aline. Even if we are dispersed all over the country, it is always a pleasure to meet.

Last but not least, I sincerely thank my family: my parents, my grandparents, my little brother whose I am very proud of. A special thank finally goes to Benoît for supporting me everyday.

# Table of Content

|   |           |
|---|-----------|
| <b>Introduction .....</b>   | <b>31</b> |
| <b>Chapter 1. State of the Art on Superhydrophobic Polymers .....</b> | <b>35</b> |
| <b>I. WETTING THEORIES.....</b>                                       | <b>36</b> |
| <b>II. SUPERHYDROPHOBICITY IN NATURE .....</b>                        | <b>40</b> |
| II.1. Superhydrophobic plant surfaces.....                            | 41        |
| II.2. Superhydrophobic animals .....                                  | 43        |
| <b>III. FABRICATION TECHNIQUES OF SUPERHYDROPHOBIC POLYMERS.....</b>  | <b>46</b> |
| III.1. Templating or Molding .....                                    | 47        |
| III.1.1. Anodic Aluminum Oxide Template .....                         | 47        |
| III.1.1.a. Direct Templating.....                                     | 47        |
| III.1.1.b. Template-assisted Polymerization .....                     | 48        |
| III.1.2. Soft Lithography .....                                       | 49        |
| III.1.2.a. Natural Masters.....                                       | 50        |
| III.1.2.b. Microfabrication.....                                      | 50        |
| III.1.3. Structured Hard Masters Replication.....                     | 51        |
| III.2. Plasma .....   | 51        |
| III.2.1. Etching Plasma .....   | 53        |
| III.2.2. Deposition Plasma .....                                      | 54        |
| III.2.3. Sputtering.....  | 57        |
| III.3. Laser .....  | 58        |
| III.4. Polymer Self-Assembly .....                                    | 59        |
| III.5. Electrochemical Polymerization .....                           | 63        |
| III.6. Electrospinning.....   | 66        |
| III.7. Precipitation and Crystallization.....                         | 71        |
| III.8. Selective Solvent.....   | 73        |
| III.9. LbL Deposition.....  | 75        |
| III.10. Combination of techniques to reach superhydrophobicity.....   | 76        |

|              |  |           |
|--------------|--|-----------|
| <b>IV.</b>   | <b>FOCUS ON FABRICATION TECHNIQUES OF SUPERHYDROPHOBIC FIBROUS</b> |           |
|              | <b>POLYMERS.....</b>   | <b>77</b> |
| <b>IV.1.</b> | <b>Fibers Coatings.....</b>  | <b>78</b> |
| IV.1.1.      | Dip-Coating.....   | 78        |
| IV.1.2.      | Polymerization.....  | 81        |
| IV.1.3.      | Other Coatings.....  | 83        |
| <b>IV.2.</b> | <b>Overview of the Techniques to Produce Superhydrophobic</b>      |           |
|              | <b>Fibrous Polymers.....</b>                                       | <b>84</b> |
|              | <b>REFERENCES.....</b>   | <b>88</b> |



|   |            |
|---|------------|
| <b>Chapter 2. Influence of Chemical and Physical Parts onto the Wetting Properties of Linear Hydrocarbon 3,4-ethylenedioxythiophene derivatives (EDOT-Hn) .....</b> | <b>107</b> |
| <b>I. SYNTHESIS OF MONOMERS .....</b>   | <b>108</b> |
| <b>II. ELECTROPOLYMERIZATION .....</b>  | <b>128</b> |
| <b>III. SURFACE CHARACTERIZATIONS.....</b>  | <b>131</b> |
| <b>III.1. Versatile Wetting and Dewetting Surfaces.....</b>   | <b>131</b> |
| III.1.1. Surface Wettability .....  | 131        |
| III.1.2. Surface Morphology and Roughness .....   | 133        |
| <b>III.2. How do the chemical and physical parts influence the surface water-repellent properties? .....</b>  | <b>138</b> |
| III.2.1. Influence of the Doping Anions .....   | 138        |
| III.2.2. Influence of the Physical Part .....   | 139        |
| III.2.3. Wenzel Roughness Factor and Cassie-Baxter Air Fraction.....  | 142        |
| <b>III.3. Superhydrophobic Surfaces from Short Alkyl Chain EDOT Derivatives .....</b>   | <b>143</b> |
| III.3.1. PEDOT-H6 .....   | 143        |
| III.3.2. PEDOT .....  | 146        |
| <b>REFERENCES.....</b>  | <b>149</b> |
| <b>Chapter 3. Fluorocarbon vs. Hydrocarbon Polymers .....</b>   | <b>151</b> |
| <b>I. EDOT-F8 vs. EDOT-HN.....</b>  | <b>152</b> |
| I.1. Monomer Synthesis.....   | 152        |
| I.2. Electrochemical Polymerization .....   | 157        |
| I.3. Surface Characterizations .....  | 158        |
| I.3.1. Surface Wettability .....  | 160        |
| I.3.2. Surface Morphology and Roughness .....   | 163        |
| <b>II. 3,4-ETHYLENEOXYTHIATHIOPHENE (EOTT) DERIVATIVES .....</b>  | <b>164</b> |
| II.1. Monomers Synthesis .....  | 164        |
| II.2. Electrochemical Polymerization .....  | 195        |
| II.3. Surface Characterizations .....   | 197        |
| II.3.1. Surface Wettability .....   | 197        |

|   |   |     |
|---|---|-----|
| II.3.2.   | Analogy in Surface Morphology.....  | 198 |
| II.4.   | Wettability Study of PEOTT-OFn with other Probe Liquids .....               | 203 |
| III.  | 3,4-PROPYLENEDIOXYTHIOPHENE (ProDOT) DERIVATIVES.....                       | 205 |
| III.1.  | Monomers Synthesis.....   | 205 |
| III.2.  | Electrochemical Polymerization .....  | 228 |
| III.3.  | Surface Characterizations.....  | 231 |
| III.3.1.  | Surface Wettability .....   | 231 |
| III.3.2.  | Surface Morphology.....   | 233 |
| III.4.  | Influence of Electrochemical Polymerization Method onto<br>PProDOT-OF4..... | 240 |
| REFERENCES.....   |   | 245 |
| Conclusion .....  |   | 249 |
| Outlooks .....  |   | 253 |
| Annexes .....   |   | 255 |
| Annex 1: Chemical Analysis Techniques for the characterization of the<br>Monomers ..... |   | 255 |
| Annex 2: Electrochemical Polymerization Technique .....                                 |   | 256 |
| Annex 3: Surface Characterizations Techniques.....                                      |   | 258 |
| Annex 4: Experimental section - Monomer synthesis.....                                  |   | 260 |
| Annex 5: Hydrocarbon conducting polymers with branched hydrophobic<br>tail .....        |   | 264 |



## List of Schemes

### Chapter 2

|  |     |
|--|-----|
| Scheme 2-1. Synthetic way to EDOT-Hn monomers ( $n = 2, 4, 6, 8, 10$ and $12$ )..... | 108 |
|--|-----|

### Chapter 3

|   |     |
|---|-----|
| Scheme 3-1. Chemical route to the fluorinated 2-perfluorooctylethane-1,2-diol .....                     | 152 |
| Scheme 3-2. Synthetic way to the fluorinated monomers.....  | 152 |
| Scheme 3-3. Synthetic way to EOTT-Fn and EOTT-Hm monomers ( $n = 4, 6, 8$ and<br>$m = 8, 10, 12$ )..... | 165 |
| Scheme 3-4. Synthetic route to ProDOT-OFn and ProDOT-OHn monomers.....                                  | 205 |

# List of Figures

## Introduction

|           |   |    |
|-----------|---|----|
| Figure 1. | Examples of chemical modifications to produce hydrophobic surfaces..... | 31 |
| Figure 2. | Thesis synoptic representation.....                                     | 34 |

## Chapter 1

|             |   |    |
|-------------|---|----|
| Figure 1-1. | Number of publications with “superhydrophobic” as enter since 1989 (Source Web of Science, October 2013).....   | 35 |
| Figure 1-2. | Liquid droplet wetting behavior and equation of Young's state.....  | 36 |
| Figure 1-3. | Liquid droplet wetting behavior in Wenzel's state and the corresponding equation. ....  | 37 |
| Figure 1-4. | Liquid droplet wetting behavior in Cassie-Baxter's state and the corresponding equation. ....   | 38 |
| Figure 1-5. | Methods to measure the contact angle hysteresis $H = \theta_a - \theta_r$ . (a) On a horizontal setup, $\theta_a$ is measured during droplet growth and $\theta_r$ is measured during its shrinkage. (b) The surface is inclined until the droplet rolls off the surface. $\theta_a$ and $\theta_r$ are measured just before the rolling occurs.....  | 39 |
| Figure 1-6. | Water droplets on a Lotus leaf (a), on the Perfoliate Knotweed leaf (c), on the Purple Setcreasea (e) and on the Rice leaf (g). SEM images of the Lotus leaf (Magnification: x 20 000) (b), of the Perfoliate Knotweed leaf (Magnification: x 10 000) (d), of the Purple Setcreasea (Magnification: x 10 000) (f) and of the Rice leaf (Magnification: x 20 000). The bars of (b), (d), (f) and (h) are 1 $\mu\text{m}$ . |    |

- The insets of (b), (d), (f) and (h) are the water contact angle on the corresponding leaves.<sup>38</sup> ..... 41
- Figure 1-7.** Water droplets on a Ramee leaf (a) and the corresponding SEM images ((b) and (c)) with different magnifications (scale bars: 100 and 5  $\mu\text{m}$ , respectively). Water droplets on a Chinese watermelon leaf (d) and the corresponding SEM images ((e) and (f)) with different magnifications (scale bars: 50 and 1  $\mu\text{m}$ , respectively). Water droplets on a Silver ragwort leaf (g) and the corresponding SEM image (h and inset of (h)) with different magnifications (scale bars: 30 and 2  $\mu\text{m}$ , respectively). The insets of (c) and (f) are the water contact angle on the corresponding leaf ( $\theta_{\text{water}} = 164 \pm 2^\circ$  and  $\theta_{\text{water}} = 159 \pm 2^\circ$ , respectively). Images (a)-(f)<sup>38</sup> and Images (g)-(h).<sup>40</sup> ..... 42
- Figure 1-8.** Morphology of *Salvinia molesta* floating leaf. a) Upper side of the leaf surface with a water droplet on it. (b-d) SEM images of the complex hair structures: b) Four multicellular hair grouped on top of an emergence and connected at the terminal end leading to an eggbeater-shaped structure. c) The terminal cell of each hair is collapsed forming a patch of four dead cells. d) The whole leaf surface is covered with nanoscale wax crystals (below) with exception of the terminal cells (above).<sup>26</sup> ..... 43
- Figure 1-9.** Hierarchical micro/nano structures on the insect wings of (a) Homoptera *Meimuna opalifera* (Walker), (b) Diptera *Tabanus chrysurus* (Lowe) and (c) Termite *Nasutitermens walker* at different magnifications. Images (a-b).<sup>39</sup> Images (c).<sup>44</sup> ..... 44
- Figure 1-10.** Hierarchical structuration of the gecko foot. (A) Macrostructure: ventral view of a tokay gecko (*G. gecko*) climbing vertical glass. (B) Mesostructure: ventral view of the foot, with adhesive lamellae (scansors) visible as overlapping pads. Note the clean appearance of the adhesive surface. (C) Microstructure:

|                     |  |    |
|---------------------|--|----|
|                     | proximal portion of single lamella, with individual setae in an array visible. (D and E) Nanostructure: single seta with branched structure at upper right, terminated in hundreds of spatula tips. <sup>45</sup> .....  | 45 |
| <b>Figure 1-11.</b> | (a) Water strider <i>Gerris</i> walking on the water surface (Scale bar: 1 mm). (b) SEM images of the hair of the water strider leg at different magnifications. <sup>47</sup> .....   | 46 |
| <b>Figure 1-12.</b> | Overview of the techniques to fabricate superhydrophobic polymers.....   | 46 |
| <b>Figure 1-13.</b> | SEM images of a Tokay Gecko ( <i>Gekko gekko</i> ) (a and c) and fabricated hierarchical PS nanohairs with high aspect ratio (b and d). Inset in (b): water contact angle of the elongated hierarchical PS nanohairs. <sup>56</sup> .....  | 48 |
| <b>Figure 1-14.</b> | Water contact angle measurements with a series of polypyrrole nanorods and Au nanoparticles after HDFT coating. Au nanoparticles size represents the diameter (d). <sup>65</sup> .....   | 49 |
| <b>Figure 1-15.</b> | Illustration of the lotus leaf replication process and creation of a superhydrophobic surface. <sup>67</sup> .....   | 50 |
| <b>Figure 1-16.</b> | Top-irradiation mode for the adhesion switch. The green light (530 nm, 30 mW.cm <sup>-2</sup> ) make the azobenzene moiety in the film into the trans state, thus the film surface shows a relatively low water adhesion. Reversibly, the UV light (365 nm, 120 mW.cm <sup>-2</sup> ) changes the azobenzene moiety into the cis state and the surface of the film shows a relatively high water adhesion. The time for UV and visible light was 6 and 30 s, respectively. <sup>78</sup> ..... | 51 |
| <b>Figure 1-17.</b> | FE-SEM images of the HDPE (a-f) and PCL (g-l) replicas with micrometer-sized irregular steps (a, b, g, h) mixed structures (c, d, i, j) and nanometer-sized curled strands (e, f, k, l) replicated from Al templates etched for 10, 20, 30, 40, 50, and 60. Insets show low magnification images (x 2 000). <sup>86</sup> .....  | 52 |



- Figure 1-18.** AFM images of untreated (A) and plasma treated PTFE samples: (B) DC-bias = -575 V,  $t = 700$  s,  $\theta_{\text{water}} = 126.2^\circ$ ,  $R_a = 242$  nm; (C) DC-bias = -750 V,  $t = 700$  s,  $\theta_{\text{water}} = 152.8^\circ$ ,  $R_a = 505$  nm.<sup>93</sup> ..... 54
- Figure 1-19.** Morphology induced by the absence (left images) or presence (right images) of the grafting step of plasma polymerization of perfluoroacrylate. AFM images (a-b) of the polymer coating (lateral scale:  $5 \times 5 \mu\text{m}$ ). SEM images of the polymer surface: top-view (c-d) and in cross section (e-f).<sup>101</sup> ..... 55
- Figure 1-20.** Liquid wettability of plasma polymeric film as a function of the number of plasma depositions.<sup>102</sup> ..... 56
- Figure 1-21.** (a) SEM images of plasma-etched PDMS after 6 min of plasma treatment. (b) AFM image of the same PDMS after a 2 min plasma treatment. (c) Image of a water droplet after hydrophobic fluorocarbon plasma. (d) AFM image of another elastomer after a 2 min plasma etching treatment.<sup>107</sup> ..... 57
- Figure 1-22.** (a) Typical SEM images of the laser-etched PDMS surface with the convex width of about  $25 \mu\text{m}$ , showing the regular arrays of microconvexes. (b) Magnified image of (a), showing the submicrometer structures on each convex. (c) High-resolution image of a single convex with width of about  $50 \mu\text{m}$  (left) and a flat PDMS surface (right).<sup>113</sup> ..... 58
- Figure 1-23.** SEM images of polymethylene films grown from HB + Si (a-b), HB + Ag/Au (c) and HB + Au (d) after polymerization.<sup>120</sup> ..... 60
- Figure 1-24.** Shape of water droplets formed on porous and nonporous polymer layers and SEM images of the superhydrophobic porous polymers. (a) Poly(butyl methacrylate-co-ethylene dimethacrylate). (b) Poly(styrene-co-divinylbenzene).<sup>122</sup> ..... 61
- Figure 1-25.** (a) SEM images of the rambutan-like hollow polyaniline (PANI) spheres. Inset is a photograph of a rambutan.<sup>127</sup> (b) SEM images of the flower-like PANI



|                     |   |
|---------------------|---|
|                     | architectures, which are composed of cross-shaped nanosheets. <sup>129</sup> (c) SEM images of the synthesized PANI at the polymerization time of 24h. <sup>130</sup> ..... 62  |
| <b>Figure 1-26.</b> | SEM images of PProDOP-F6 with magnifications of (a) x 5 000, (b) x 25 000 and of PEDOT-F6 with magnifications of (d) x 5 000 and (e) x 25 000. (Scale bars: 1 $\mu$ m). (c) and (f): hexadecane droplets on the corresponding surface. <sup>140</sup> ..... 64  |
| <b>Figure 1-27.</b> | Surface morphology comparison between PEOT-F4 and PEDOT-F4, electrodeposited with the same conditions. <sup>143</sup> ..... 65  |
| <b>Figure 1-28.</b> | SEM images of polypyrrole nanofibers arrays after (a) 10, (b) 20, (c) 30 and (d) 40 CV scanning cycles. <sup>151</sup> ..... 66   |
| <b>Figure 1-29.</b> | SEM images of the electrospun PS fibers formed from 30 wt % of PS in THF/DMF solvent (1:3). <sup>183</sup> ..... 68   |
| <b>Figure 1-30.</b> | SEM and TEM images of coaxially electrospun core-sheath fiber mat 1 wt % Teflon / 7 wt % PVDF. SEM images with magnifications of (a,f) x 10 000, (b) x 20 000 and (e) x 2 000 and TEM images with a magnification of (c, d) x 30 000. The difference in contrast is due to the difference of chemical structure between Teflon (core, dark) and PVDF (sheath, clear). (e, f) SEM images of core-sheath fiber sample after sheath removal. <sup>186</sup> ..... 70 |
| <b>Figure 1-31.</b> | SEM images of <i>P. aeruginosa</i> PAO1 colonization on (A) unmodified PVC ( $\theta_{\text{water}} = 80^\circ$ ); (B) 25 % (v/v) ethanol-treated PVC ( $\theta_{\text{water}} = 113^\circ$ ); and (C) 35 % (v/v) ethanol-treated PVC ( $\theta_{\text{water}} = 150^\circ$ ) samples at different incubation time points (scale bar: 10 $\mu$ m). <sup>204</sup> ..... 72  |
| <b>Figure 1-32.</b> | SEM images of the as-prepared porous film with different magnifications (Scale bars: (a) 1 $\mu$ m and (b) 100 nm). <sup>208</sup> ..... 73   |
| <b>Figure 1-33.</b> | (A-C) SEM images of 100-bilayer films fabricated from PEI and PVDMAoligo that were (A) unmodified, (B) treated with decylamine; or (C) treated with HDFA. The images were acquired after soaking the unmodified film in water   |

|                     |   |    |
|---------------------|---|----|
|                     | for 1 week and the decylamine-treated films in water for 6 weeks (Scale bars: 2 $\mu$ m). (D-F) Images of water droplets (4 $\mu$ L) on the corresponding surfaces. <sup>215</sup> .....  | 75 |
| <b>Figure 1-34.</b> | Techniques to produce Superhydrophobic Fibrous Polymers .....   | 77 |
| <b>Figure 1-35.</b> | SEM images of (a) untreated cotton textile surface and (b) cotton surface treated with 0.5 wt% amino-SiO <sub>2</sub> , 0.5 wt% stearic acid and 0.5 vol% PFTDS. The inset of (b) is the image of static water droplets on the surface. <sup>231</sup> .....  | 79 |
| <b>Figure 1-36.</b> | Large-scale SEM image of the raw paper (a) and the magnified image of a single fiber (b). Large-scale SEM images of the fluorinated waterborne epoxy resin emulsion coated paper (c) and the magnified image of a single fiber (d). The insets in images (a) and (c) are the water droplet onto the corresponding surfaces. <sup>237</sup> .....  | 80 |
| <b>Figure 1-37.</b> | SEM images of the surface of uncoated fabric (a) and coated surface (b). Inset is a photo of water droplet on the sample. <sup>247</sup> .....  | 81 |
| <b>Figure 1-38.</b> | (a) Colored water droplets are laying onto the area of a cellulose sheet treated with PECA (defined by the red line), whereas they are absorbed by its untreated area. (c) SEM image showing the surface of a cellulose fiber roughened by submicrometer (<200 nm) PTFE particles mixed with PECA (20.0 wt% PTFE in PECA) to fabricate super water repellent cellulose sheets. <sup>248</sup> ..... | 82 |
| <b>Figure 1-39.</b> | (a) Reversible wettability change of the PMETAC films by repeated counterion exchange between PFO and SCN <sup>-</sup> . (b) The photographs of water droplets on PMETAC brush films bearing PFO and SCN <sup>-</sup> respectively, and the adhesive properties of PMETAC brush film bearing PFO. <sup>251</sup> .....  | 83 |
| <b>Figure 1-40.</b> | SEM images of (a) pristine cotton fiber and cotton fibers coated with (PAH-N <sub>3</sub> /silica-N <sub>3</sub> ) <sub>n</sub> multilayers: (b) n = 1.5, (c) n = 3.5 and (d) n = 5.5. <sup>256</sup> .....   | 84 |
| <b>Figure 1-41.</b> | Synthetic route to all the monomers described in the following studies.....   | 87 |

## Chapter 2

|              |  |     |
|--------------|--|-----|
| Figure 2-1.  | Chemical structure of monomers in the present study (n = 2; 4; 6; 8; 10; 12)....   | 107 |
| Figure 2-2.  | Proton attribution for EDOT-H2. ....   | 110 |
| Figure 2-3.  | Carbon attribution for EDOT-H2. ....   | 111 |
| Figure 2-4.  | Proton attribution for EDOT-H4. ....   | 113 |
| Figure 2-5.  | Carbon attribution for EDOT-H4. ....   | 114 |
| Figure 2-6.  | Proton attribution for EDOT-H6. ....   | 116 |
| Figure 2-7.  | Carbon attribution for EDOT-H6. ....   | 117 |
| Figure 2-8.  | Proton attribution for EDOT-H8. ....   | 119 |
| Figure 2-9.  | Carbon attribution for EDOT-H8 ....  | 120 |
| Figure 2-10. | Proton attribution for EDOT-H10.....   | 122 |
| Figure 2-11. | Carbon attribution for EDOT-H10.....   | 123 |
| Figure 2-12. | Proton attribution for EDOT-H12.....   | 125 |
| Figure 2-13. | Carbon attribution for EDOT-H12.....   | 126 |
| Figure 2-14. | Cyclic voltammograms of EDOT-H8 (0.01 M) on a Pt electrode recorded in 0.1 M Bu <sub>4</sub> NPF <sub>6</sub> /Acetonitrile with a scan rate of 20 mV.s <sup>-1</sup> .....                              | 129 |
| Figure 2-15. | Cyclic voltammogram of PEDOT-Hn with ascan rate of 20 mV.s <sup>-1</sup> in a monomer-free solution with 0.1 M of Bu <sub>4</sub> NPF <sub>6</sub> /Acetonitrile.....                                    | 130 |
| Figure 2-16. | Static contact angles of water and diiodomethane as a function of the alkyl chain length.....  | 132 |
| Figure 2-17. | SEM images of a) PEDOT-H2, b) PEDOT-H4, c) PEDOT-H6 and d) PEDOT-H8 with a magnification of x 5 000 (Salt: Bu <sub>4</sub> NPF <sub>6</sub> ; Solvent: Acetonitrile; Qs ≈ 200 mC.cm <sup>-2</sup> )..... | 134 |



|                     |   |     |
|---------------------|---|-----|
| <b>Figure 2-18.</b> | SEM images of PEDOT-H10 (left with a magnification of a) x 250, b) x 5 000 and c) x 10 000) and PEDOT-H12 (right with a magnification of a) x 250, b) x 5 000 and c) x 10 000) (Salt: $\text{Bu}_4\text{NPF}_6$ ; Solvent: Acetonitrile; $Q_s \approx 200 \text{ mC.cm}^{-2}$ )....   | 135 |
| <b>Figure 2-19.</b> | Static water contact angles as a function of the deposition charge.....   | 137 |
| <b>Figure 2-20.</b> | Mean arithmetic roughness ( $R_a$ ) as a function of the deposition charge.....   | 137 |
| <b>Figure 2-21.</b> | Wetting behavior of PEDOT-Hn series depending on their oxidation state.....   | 139 |
| <b>Figure 2-22.</b> | SEM images of PEDOT-H10 obtained when electropolymerized in various solvents: a) propylene carbonate, b) benzonitrile, c) nitrobenzene, d) chloroform and e) dichloromethane (Magnification: x 10 000; Salt: $\text{Bu}_4\text{NPF}_6$ ; $Q_s = 200 \text{ mC.cm}^{-2}$ ).....  | 140 |
| <b>Figure 2-23.</b> | Static water contact angle for PEDOT-H10 as a function of the deposition charge in various solvents.....  | 141 |
| <b>Figure 2-24.</b> | Schematic representation of the influence of chemical and physical parts on the water wetting properties for PEDOT-Hn. (Salt: $\text{Bu}_4\text{NPF}_6$ ; $Q_s \approx 100 \text{ mC.cm}^{-2}$ ).<br>.....  | 142 |
| <b>Figure 2-25.</b> | SEM images of PEDOT-H6 electropolymerized with various supporting electrolyte: a) $\text{NaClO}_4$ , b) $\text{Bu}_4\text{NClO}_4$ , c) $\text{Bu}_4\text{NBF}_4$ , d) $\text{Bu}_4\text{NCF}_3\text{SO}_3$ , e) $\text{Bu}_4\text{NC}_4\text{F}_9\text{SO}_3$ and f) $\text{Bu}_4\text{NC}_8\text{F}_{17}\text{SO}_3$ (Magnification x 5 000; solvent: Acetonitrile; $Q_s = 200 \text{ mC.cm}^{-2}$ )..... | 145 |
| <b>Figure 2-26.</b> | SEM images of PEDOT electropolymerized with two different fluorinated salts: a) $\text{Bu}_4\text{NC}_4\text{F}_9\text{SO}_3$ and b) $\text{Bu}_4\text{NC}_8\text{F}_{17}\text{SO}_3$ (Magnification x 10 000; solvent: acetonitrile; $Q_s = 200 \text{ mC.cm}^{-2}$ ).....   | 147 |

## Chapter 3

|                    |  |     |
|--------------------|--|-----|
| <b>Figure 3-1.</b> | Chemical structure of the monomers of Chapter 3..... | 151 |
| <b>Figure 3-2.</b> | Protons attribution for EDOT-F8.....                 | 153 |

|                     |   |     |
|---------------------|---|-----|
| <b>Figure 3-3.</b>  | Carbons attribution for EDOT-F8. ....   | 154 |
| <b>Figure 3-4.</b>  | Fluorines attribution for EDOT-F8. ....   | 155 |
| <b>Figure 3-5.</b>  | Cyclic voltammograms of EDOT-F8 on a Pt electrode recorded in 0.1 M<br>Bu <sub>4</sub> NPF <sub>6</sub> /acetonitrile. ....   | 158 |
| <b>Figure 3-6.</b>  | Influence of the deposition charge (Q <sub>s</sub> ) on the static contact angle of water<br>(blue) and diidomethane (red) for PEDOT-F8. ....   | 159 |
| <b>Figure 3-7.</b>  | SEM images of the films obtained by electrodeposition of PEDOT-F8 and<br>using different deposition charges: a) Q <sub>s</sub> = 25 mC.cm <sup>-2</sup> ; b) Q <sub>s</sub> = 50 mC.cm <sup>-2</sup> ;<br>c) 100 mC.cm <sup>-2</sup> ; d) 200 mC.cm <sup>-2</sup> ; e) 300 mC.cm <sup>-2</sup> (Magnification: x 5 000). .... | 161 |
| <b>Figure 3-8.</b>  | AFM images of the films obtained by electrodeposition of PEDOT-F8 films at<br>two different scales. The analyzed area are: a) 50 μm x 50 μm and b) 13 μm x<br>13 μm (Q <sub>s</sub> = 100 mC.cm <sup>-2</sup> ). ....   | 162 |
| <b>Figure 3-9.</b>  | Arithmetic roughness parameter (Ra) of PEDOT-F8 as a function of the<br>deposition charge. ....   | 163 |
| <b>Figure 3-10.</b> | Proton attribution for EOTT-OH. ....  | 167 |
| <b>Figure 3-11.</b> | Carbon attribution for EOTT-OH. ....  | 168 |
| <b>Figure 3-12.</b> | Proton attribution for EOTT-OF4. ....   | 170 |
| <b>Figure 3-13.</b> | Carbon attribution for EOTT-OF4. ....   | 171 |
| <b>Figure 3-14.</b> | Fluorine attribution for EOTT-OF4. ....   | 172 |
| <b>Figure 3-15.</b> | Proton attribution for EOTT-F6. ....  | 174 |
| <b>Figure 3-16.</b> | Carbon attribution for EOTT-OF6. ....   | 175 |
| <b>Figure 3-17.</b> | Fluorine attribution for EOTT-OF6. ....   | 176 |
| <b>Figure 3-18.</b> | Proton attribution for EOTT-OF8. ....   | 178 |
| <b>Figure 3-19.</b> | Carbon attribution for EOTT-OF8. ....   | 179 |
| <b>Figure 3-20.</b> | Fluorine attribution for EOTT-OF8. ....   | 180 |
| <b>Figure 3-21.</b> | Protons attribution for EOTT-OH4. ....  | 182 |



|              |  |     |
|--------------|--|-----|
| Figure 3-22. | Carbons attribution for EOTT-OH4.....  | 183 |
| Figure 3-23. | Protons attribution for EOTT-OH6.....  | 184 |
| Figure 3-24. | Carbons attribution for EOTT-OH6.....  | 185 |
| Figure 3-25. | Protons attribution for EOTT-OH8.....  | 186 |
| Figure 3-26. | Carbons attribution for EOTT-OH8.....  | 187 |
| Figure 3-27. | Protons attribution for EOTT-OH10.....   | 189 |
| Figure 3-28. | Carbons attribution for EOTT-OH10.....   | 190 |
| Figure 3-29. | Protons attribution for EOTT-OH12.....   | 191 |
| Figure 3-30. | Carbons attribution for EOTT-OH12.....   | 192 |
| Figure 3-31. | Cyclic voltammogram of a) PEOTT-OF6 and b) PEOTT-OH10 (0.01 M) on a Pt electrode recorded in Bu <sub>4</sub> NPF <sub>6</sub> /acetonitrile with a scan rate of 20 mV.s <sup>-1</sup> . Last voltammogram cycle of c) PEOTT-OF6 and d) PEOTT-OH10 recorded in a monomer-free solution with Bu <sub>4</sub> NPF <sub>6</sub> /acetonitrile..... | 197 |
| Figure 3-32. | SEM images of PEOTT derivatives substituted with various fluorocarbon or hydrocarbon chains (Magnification: x 10 000).....   | 200 |
| Figure-3 33. | Optical profilometer images of a) PEOTT-OF4, b) PEOTT-OF6, c) PEOTT-OF8, d) PEOTT-OH8, e) PEOTT-OH10 and f) PEOTT-OH12. (Scale bar: from -10 (dark blue) to +20 (red) μm).....   | 202 |
| Figure 3-34. | Static contact angle of water, diiodomethane and hexadecane as a function of the fluorinated chain length.....   | 203 |
| Figure 3-35. | Protons attribution for ProDOT-OF4.....  | 207 |
| Figure 3-36. | Carbons attribution for ProDOT-OF4.....  | 208 |
| Figure 3-37. | Fluorine attribution for PEDOT-OF4.....  | 209 |
| Figure 3-38. | Protons attribution for ProDOT-OF6.....  | 211 |
| Figure 3-39. | Carbons attribution for ProDOT-OF6.....  | 212 |
| Figure 3-40. | Fluorine attribution for ProDOT-OF6.....   | 213 |

|                     |   |     |
|---------------------|---|-----|
| <b>Figure 3-41.</b> | Protons attribution for ProDOT-OF8.....   | 215 |
| <b>Figure 3-42.</b> | Carbons attribution for ProDOT-OF8.....   | 216 |
| <b>Figure 3-43.</b> | Fluorine attribution for ProDOT-OF8.....  | 217 |
| <b>Figure 3-44.</b> | Protons attribution for ProDOT-OH4.....   | 219 |
| <b>Figure 3-45.</b> | Carbons attribution for ProDOT-OH4.....   | 220 |
| <b>Figure 3-46.</b> | Protons attribution for ProDOT-OH6.....   | 221 |
| <b>Figure 3-47.</b> | Carbons attribution for ProDOT-OH6.....   | 223 |
| <b>Figure 3-48.</b> | Protons attribution for ProDOT-OH8.....   | 225 |
| <b>Figure 3-49.</b> | Carbons attribution for ProDOT-OH8.....   | 226 |
| <b>Figure 3-50.</b> | Cyclic voltammograms of PProDOT-OF <sub>n</sub> in a) acetonitrile and in<br>b) dichloromethane. Cyclic voltammoogram of PProDOT-OH <sub>n</sub> in c) acetonitrile<br>and in d) dichloromethane.....   | 230 |
| <b>Figure 3-51.</b> | SEM images of PProDOT-OF <sub>4</sub> in a) acetonitrile and a') in dichloromethane;<br>PProDOT-OF <sub>6</sub> in b) acetonitrile and b') dichloromethane; PProDOT-OF <sub>8</sub> in<br>c) acetonitrile and c') dichloromethane ( $Q_s = 100 \text{ mC.cm}^{-2}$ ).....                     | 236 |
| <b>Figure 3-52.</b> | SEM images of a) PProDOT-OH <sub>4</sub> , b) PProDOT-OH <sub>6</sub> and c) PProDOT-OH <sub>8</sub><br>electrodeposited in acetonitrile (Magnification x 250. The corner insets<br>show the zoomed-out images with a magnification of x 5 000 ( $Q_s = 100$<br>$\text{mC.cm}^{-2}$ )). ..... | 236 |
| <b>Figure 3-53.</b> | SEM images of a) PProDOT-OH <sub>4</sub> , b) PProDOT-OH <sub>6</sub> and c) PProDOT-OH <sub>8</sub> ,<br>electrodeposited in dichloromethane (Magnification x 10 000;<br>$Q_s = 100 \text{ mC.cm}^{-2}$ ).....   | 237 |
| <b>Figure 3-54.</b> | SEM images of PProDOT-OF <sub>4</sub> electropolymerized in a) acetonitrile and in<br>b) dichloromethane (Magnification x 2 500; $Q_s = 100 \text{ mC.cm}^{-2}$ ).....  | 239 |

|                     |   |     |
|---------------------|---|-----|
| <b>Figure 3-55.</b> | Water (blue), diiodomethane (red) and hexadecane (green) static contact angles of PProDOT-OF4 polymer films as a function of the number of scans with a scan rate of a) 0.02 V.s <sup>-1</sup> and b) 0.1 V.s <sup>-1</sup> .....   | 240 |
| <b>Figure 3-56.</b> | SEM images of PProDOT-OF4 obtained by cyclic voltammetry with a scan rate of a) 0.02 V.s <sup>-1</sup> and b) 0.1 V.s <sup>-1</sup> (Magnification: x 250). The corner insets show the zoomed-out images with a magnification of x 10 000 (acetonitrile; supporting electrolyte: Bu <sub>4</sub> NPF <sub>6</sub> ; number of scans: 10)..... | 242 |
| <b>Figure 3-57.</b> | Arithmetic surface roughness (Ra) as a function of the scan rate and the number of CV scans.....  | 242 |

## Conclusion

|                  |   |     |
|------------------|---|-----|
| <b>Figure 1.</b> | General structures of the monomers synthesized in this work.....  | 249 |
| <b>Figure 2.</b> | Influence of the chemical and physical part on the wetting properties for PEDOT-Hn (Qs = 100 mC.cm <sup>-2</sup> ).....     | 250 |
| <b>Figure 3.</b> | SEM images of PEOTT derivatives substituted with various fluorocarbon or hydrocarbon chains (Magnification: x 10 000). .... | 251 |
| <b>Figure 4.</b> | SEM images of superhydrophobic PProDOT-OH6 polymer films with a magnification of x 250 (left) and x 5 000 (right). ....     | 252 |

## Outlooks

|                  |  |     |
|------------------|--|-----|
| <b>Figure 1.</b> | Chemical structure of the studied monomers (n = 1; 2; 3 and m = 1; 2; 3; 4; 5). .. | 253 |
|------------------|--|-----|

## Annexes

|                  |   |     |
|------------------|---|-----|
| <b>Figure 1.</b> | Protons attribution for EDOT-OCO-H1H1. .... | 265 |
|------------------|---|-----|

|                   |  |     |
|-------------------|--|-----|
| <b>Figure 2.</b>  | Carbons attribution for EDOT-OCO-H1H1. ....  | 266 |
| <b>Figure 3.</b>  | Protons attribution for EDOT-OCO-H2H2.....   | 268 |
| <b>Figure 4.</b>  | Carbons attribution for EDOT-OCO-H2H2. ....  | 269 |
| <b>Figure 5.</b>  | Protons attribution for EDOT-OCO-H3H3.....   | 271 |
| <b>Figure 6.</b>  | Carbons attribution for EDOT-OCO-H3H3. ....  | 272 |
| <b>Figure 7.</b>  | Protons attribution for EDOT-OCO-H1H2.....   | 274 |
| <b>Figure 8.</b>  | Carbons attribution for EDOT-OCO-H1H2. ....  | 275 |
| <b>Figure 9.</b>  | Protons attribution for EDOT-OCO-H1H3.....   | 277 |
| <b>Figure 10.</b> | Carbons attribution for EDOT-OCO-H1H3. ....  | 278 |
| <b>Figure 11.</b> | Protons attribution for EDOT-OCO-H1H4.....   | 280 |
| <b>Figure 12.</b> | Carbons attribution for EDOT-OCO-H1H4. ....  | 281 |
| <b>Figure 13.</b> | Protons attribution for EDOT-OCO-H1H5.....   | 283 |
| <b>Figure 14.</b> | Carbons attribution for EDOT-OCO-H1H5. ....  | 284 |
| <b>Figure 15.</b> | Water contact angles of PEDOT-OCO-HnHm as a function of the deposition charge Qs.....  | 287 |
| <b>Figure 16.</b> | Arithmetic roughness (Ra) of PEDOT-OCO-HnHm as a function of the deposition charge Qs.....   | 287 |
| <b>Figure 17.</b> | SEM images of a) PEDOT-OCO-H1H1, b) PEDOT-OCO-H2H2, c) PEDOT-OCO-H3H3 with a magnification of x 250. The insets are the zoomed-out images with a magnification of x 5 000.....   | 288 |
| <b>Figure 18.</b> | SEM images of a) PEDOT-OCO-H1H2, b) PEDOT-OCO-H1H3, c) PEDOT-OCO-H1H4 and d) PEDOT-OCO-H1H5 with a magnification of x 250. The insets are the zoomed out images with a magnification of x 5 000. (Qs = 200 mC.cm <sup>-2</sup> for images a and b; Qs = 100 mC.cm <sup>-2</sup> for images c and d)..... | 289 |



# List of Tables

## Chapter 1

|                   |  |    |
|-------------------|--|----|
| <b>Table 1-1.</b> | Effect of the polymer concentration in electrospinning solution on the morphology and wettability properties. <sup>158</sup> ..... | 67 |
| <b>Table 1-2.</b> | Double techniques employed in the literature to obtain superhydrophobic polymers.....  | 76 |
| <b>Table 1-3.</b> | List of the different techniques to produce vertical or horizontal polymer fibers and the references using these techniques .....  | 85 |

## Chapter 2

|                    |   |     |
|--------------------|---|-----|
| <b>Table 2-1.</b>  | Characteristics of synthesized EDOT-Hn monomers.....            | 109 |
| <b>Table 2-2.</b>  | <sup>1</sup> H NMR data of EDOT-H2 in CDCl <sub>3</sub> .....   | 110 |
| <b>Table 2-3.</b>  | <sup>13</sup> C NMR data of EDOT-H2 in CDCl <sub>3</sub> . .... | 111 |
| <b>Table 2-4.</b>  | MS data of EDOT-H2. ....  | 112 |
| <b>Table 2-5.</b>  | <sup>1</sup> H NMR data of EDOT-H4 in CDCl <sub>3</sub> .....   | 113 |
| <b>Table 2-6.</b>  | <sup>13</sup> C NMR data of EDOT-H4 in CDCl <sub>3</sub> . .... | 114 |
| <b>Table 2-7.</b>  | MS data of EDOT-H4. ....  | 115 |
| <b>Table 2-8.</b>  | <sup>1</sup> H NMR data of EDOT-H6 in CDCl <sub>3</sub> .....   | 116 |
| <b>Table 2-9.</b>  | <sup>13</sup> C NMR data of EDOT-H6 in CDCl <sub>3</sub> . .... | 117 |
| <b>Table 2-10.</b> | MS data of EDOT-H6 .....  | 118 |
| <b>Table 2-11.</b> | <sup>1</sup> H NMR data of EDOT-H8 in CDCl <sub>3</sub> .....   | 119 |
| <b>Table 2-12.</b> | <sup>13</sup> C NMR data of EDOT-H8 in CDCl <sub>3</sub> . .... | 120 |



|                    |   |     |
|--------------------|---|-----|
| <b>Table 2-13.</b> | MS data of EDOT-H8.....   | 121 |
| <b>Table 2-14.</b> | $^1\text{H}$ NMR data of EDOT-H10 in $\text{CDCl}_3$ .....  | 122 |
| <b>Table 2-15.</b> | $^{13}\text{C}$ NMR data of EDOT-H10 in $\text{CDCl}_3$ .....   | 123 |
| <b>Table 2-16.</b> | MS data of EDOT-H10. ....   | 124 |
| <b>Table 2-17.</b> | $^1\text{H}$ NMR data of EDOT-H12 in $\text{CDCl}_3$ .....  | 125 |
| <b>Table 2-18.</b> | $^{13}\text{C}$ NMR data of EDOT-H12 in $\text{CDCl}_3$ .....   | 126 |
| <b>Table 2-19.</b> | MS data of EDOT-H12. ....   | 127 |
| <b>Table 2-20.</b> | Electrochemical data for EDOT-Hn. ....  | 128 |
| <b>Table 2-21.</b> | Electrochemical data of PEDOT-Hn polymers.....  | 129 |
| <b>Table 2-22.</b> | Static contact angles of the PEDOT-Hn films (Salt: $\text{Bu}_4\text{NPF}_6$ ; Solvent: Acetonitrile; $Q_s \approx 100 \text{ mC.cm}^{-2}$ )..... | 132 |
| <b>Table 2-23.</b> | Roughness data for PEDOT-Hn (Salt: $\text{Bu}_4\text{NPF}_6$ ; Solvent: Acetonitrile; $Q_s \approx 100 \text{ mC.cm}^{-2}$ ).....                 | 136 |
| <b>Table 2-24.</b> | Water static contact angles of PEDOT-H6 as a function of the supporting electrolyte and the deposition charge. ....                               | 144 |
| <b>Table 2-25.</b> | Roughness parameters ( $R_a/R_q$ ) in $\mu\text{m}$ of PEDOT-H6 as a function of the supporting electrolyte and the deposition charge.....        | 145 |
| <b>Table 2-26.</b> | Water static contact angles of PEDOT as a function of the supporting electrolyte and the deposition charge. ....                                  | 146 |
| <b>Table 2-27.</b> | Roughness parameters ( $R_a/R_q$ ) in $\mu\text{m}$ of PEDOT as a function of the supporting electrolyte and the deposition charge.....           | 147 |

## Chapter 3

|                   |   |     |
|-------------------|---|-----|
| <b>Table 3-1.</b> | $^1\text{H}$ NMR data for EDOT-F8 in $\text{CDCl}_3$ .....    | 153 |
| <b>Table 3-2.</b> | $^{13}\text{C}$ NMR data for EDOT-F8 in $\text{CDCl}_3$ ..... | 154 |
| <b>Table 3-3.</b> | $^{19}\text{F}$ NMR data for EDOT-F8 in $\text{CDCl}_3$ ..... | 155 |

|             |  |     |
|-------------|--|-----|
| Table 3-4.  | MS data for EDOT-F8.....   | 156 |
| Table 3-5.  | Dynamic contact angle of water as a function of the deposition charge.....                               | 159 |
| Table 3-6.  | Characteristics of synthesized EOTT-OH, EOTT-OF <sub>n</sub> and EOTT-OH <sub>m</sub> monomers.<br>..... | 166 |
| Table 3-7.  | <sup>1</sup> H NMR data of EOTT-OH in CDCl <sub>3</sub> .....  | 167 |
| Table 3-8.  | <sup>13</sup> C NMR data of EOTT-OH in CDCl <sub>3</sub> .....   | 168 |
| Table 3-9.  | MS data of EOTT-OH .....   | 169 |
| Table 3-10. | <sup>1</sup> H NMR data of EOTT-OF <sub>4</sub> in CDCl <sub>3</sub> .....                               | 170 |
| Table 3-11. | <sup>13</sup> C NMR data of EOTT-OF <sub>4</sub> in CDCl <sub>3</sub> .....                              | 171 |
| Table 3-12. | <sup>19</sup> F NMR data of EOTT-OF <sub>4</sub> in CDCl <sub>3</sub> .....                              | 172 |
| Table 3-13. | MS data of EOTT-F <sub>4</sub> .....   | 173 |
| Table 3-14. | <sup>1</sup> H NMR data of EOTT-OF <sub>6</sub> in CDCl <sub>3</sub> .....                               | 174 |
| Table 3-15. | <sup>13</sup> C NMR data of EOTT-OF <sub>6</sub> in CDCl <sub>3</sub> .....                              | 175 |
| Table 3-16. | <sup>19</sup> F NMR data of EOTT-OF <sub>6</sub> in CDCl <sub>3</sub> .....                              | 176 |
| Table 3-17. | MS data of EOTT-OF <sub>6</sub> .....  | 177 |
| Table 3-18. | <sup>1</sup> H NMR data of EOTT-OF <sub>8</sub> in CDCl <sub>3</sub> .....                               | 178 |
| Table 3-19. | <sup>13</sup> C NMR data of EOTT-OF <sub>8</sub> in CDCl <sub>3</sub> .....                              | 179 |
| Table 3-20. | <sup>19</sup> F NMR data of EOTT-OF <sub>8</sub> in CDCl <sub>3</sub> .....                              | 180 |
| Table 3-21. | MS data of EOTT-OF <sub>8</sub> .....  | 181 |
| Table 3-22. | <sup>1</sup> H NMR data of EOTT-OH <sub>4</sub> in CDCl <sub>3</sub> .....                               | 182 |
| Table 3-23. | <sup>13</sup> C NMR data of EOTT-OH <sub>4</sub> in CDCl <sub>3</sub> .....                              | 183 |
| Table 3-24. | <sup>1</sup> H NMR data of EOTT-OH <sub>6</sub> in CDCl <sub>3</sub> .....                               | 184 |
| Table 3-25. | <sup>13</sup> C NMR data of EOTT-OH <sub>6</sub> in CDCl <sub>3</sub> .....                              | 185 |
| Table 3-26. | <sup>1</sup> H NMR data of EOTT-OH <sub>8</sub> in CDCl <sub>3</sub> .....                               | 186 |
| Table 3-27. | <sup>13</sup> C NMR data of EOTT-OH <sub>8</sub> in CDCl <sub>3</sub> .....                              | 187 |
| Table 3-28. | MS data of EOTT-OH <sub>8</sub> .....  | 188 |

|             |  |     |
|-------------|--|-----|
| Table 3-29. | $^1\text{H}$ NMR data of EOTT-OH10 in $\text{CDCl}_3$ .....  | 189 |
| Table 3-30. | $^{13}\text{C}$ NMR data of EOTT-OH10 in $\text{CDCl}_3$ .....   | 190 |
| Table 3-31. | MS data of EOTT-OH10.....  | 191 |
| Table 3-32. | $^1\text{H}$ NMR data of EOTT-OH12 in $\text{CDCl}_3$ .....  | 192 |
| Table 3-33. | $^{13}\text{C}$ NMR data of EOTT-OH12 in $\text{CDCl}_3$ .....   | 193 |
| Table 3-34. | MS data of EOTT-OH12.....  | 194 |
| Table 3-35. | Electrochemical data of PEOOT-OFn and PEOTT-OHm polymers .....   | 195 |
| Table 3-36. | Static and dynamic contact angles on PEOTT-Fn and PEOTT-OHm surfaces<br>electrodeposited on gold substrate by cyclic voltammetry (salt: $\text{Bu}_4\text{NPF}_6$ ;<br>solvent: acetonitrile). ..... | 198 |
| Table 3-37. | Roughness data for PEOTT-OFn and PEOTT-OHm polymers. ....  | 202 |
| Table 3-38. | Characteristics of synthesized ProDOT derivatives.....   | 206 |
| Table 3-39. | $^1\text{H}$ NMR data for ProDOT-OF4 in $\text{CDCl}_3$ .....  | 207 |
| Table 3-40. | $^{13}\text{C}$ NMR data for ProDOT-OF4 in $\text{CDCl}_3$ .....   | 208 |
| Table 3-41. | $^{19}\text{F}$ NMR data for ProDOT-OF4 in $\text{CDCl}_3$ .....   | 209 |
| Table 3-42. | MS data for ProDOT-OF4.....  | 210 |
| Table 3-43. | $^1\text{H}$ NMR data for ProDOT-OF6 in $\text{CDCl}_3$ .....  | 211 |
| Table 3-44. | $^{13}\text{C}$ NMR data for ProDOT-OF6 in $\text{CDCl}_3$ .....   | 212 |
| Table 3-45. | $^{19}\text{F}$ NMR data for ProDOT-OF6 in $\text{CDCl}_3$ .....   | 213 |
| Table 3-46. | MS data for ProDOT-OF6 .....   | 214 |
| Table 3-47. | $^1\text{H}$ NMR data for ProDOT-OF8 in $\text{CDCl}_3$ .....  | 215 |
| Table 3-48. | $^{13}\text{C}$ NMR data for ProDOT-OF8 in $\text{CDCl}_3$ .....   | 216 |
| Table 3-49. | $^{19}\text{F}$ NMR data for ProDOT-OF8 in $\text{CDCl}_3$ .....   | 217 |
| Table 3-50. | MS data for ProDOT-OF8 .....   | 218 |
| Table 3-51. | $^1\text{H}$ NMR data for ProDOT-OH4 in $\text{CDCl}_3$ .....  | 219 |
| Table 3-52. | $^{13}\text{C}$ NMR data for ProDOT-OH4 in $\text{CDCl}_3$ .....   | 220 |

|                    |  |     |
|--------------------|--|-----|
| <b>Table 3-53.</b> | MS data for ProDOT-OH4 .....   | 221 |
| <b>Table 3-54.</b> | $^1\text{H}$ NMR data for ProDOT-OH6 in $\text{CDCl}_3$ .....  | 222 |
| <b>Table 3-55.</b> | $^{13}\text{C}$ NMR data for ProDOT-OH6 in $\text{CDCl}_3$ .....   | 223 |
| <b>Table 3-56.</b> | MS data for ProDOT-OH6 .....   | 224 |
| <b>Table 3-57.</b> | $^1\text{H}$ NMR data for ProDOT-OH8 in $\text{CDCl}_3$ .....  | 225 |
| <b>Table 3-58.</b> | $^{13}\text{C}$ NMR data for ProDOT-OH8 in $\text{CDCl}_3$ .....   | 226 |
| <b>Table 3-59.</b> | MS data for ProDOT-OH8 .....   | 227 |
| <b>Table 3-60.</b> | Oxidation potential of the monomers (V vs. SCE) as a function of the electropolymerization solvent.....  | 229 |
| <b>Table 3-61.</b> | Electrochemical data of PProDOT-OFn and PProDOT-OHn in acetonitrile (all potentials are in V vs. SCE). .....   | 230 |
| <b>Table 3-62.</b> | Water-repellent properties of the PProDOT polymers as a function of the electropolymerization solvent for an electrodeposited charge of $Q_s = 100 \text{ mC.cm}^{-2}$ ..... | 232 |
| <b>Table 3-63.</b> | Diiodomethane and Hexadecane static contact angles of PProDOT-OFn polymers ( $Q_s = 100 \text{ mC.cm}^{-2}$ ).....   | 233 |
| <b>Table 3-64.</b> | Roughness parameters ( $R_a$ and $R_q$ ) in $\mu\text{m}$ of PProDOT derivatives depending on the electropolymerized solvent.....  | 239 |

## Annexes

|                 |  |     |
|-----------------|--|-----|
| <b>Table 1.</b> | Characteristics of synthesized EDOT-OCO-HnHm monomers. ....        | 268 |
| <b>Table 2.</b> | $^1\text{H}$ NMR data of EDOT-OCO-H1H1 in $\text{CDCl}_3$ .....    | 269 |
| <b>Table 3.</b> | $^{13}\text{C}$ NMR data of EDOT-OCO-H1H1 in $\text{CDCl}_3$ ..... | 270 |
| <b>Table 4.</b> | MS data of EDOT-OCO-H1H1. ....                                     | 271 |
| <b>Table 5.</b> | $^1\text{H}$ NMR data of EDOT-OCO-H2H2 in $\text{CDCl}_3$ .....    | 272 |
| <b>Table 6.</b> | $^{13}\text{C}$ NMR data of EDOT-OCO-H2H2 in $\text{CDCl}_3$ ..... | 273 |



|                  |   |     |
|------------------|---|-----|
| <b>Table 7.</b>  | MS data of EDOT-OCO-H2H2.....   | 274 |
| <b>Table 8.</b>  | <sup>1</sup> H NMR data of EDOT-OCO-H3H3 in CDCl <sub>3</sub> .....   | 275 |
| <b>Table 9.</b>  | <sup>13</sup> C NMR data of EDOT-OCO-H3H3 in CDCl <sub>3</sub> . .... | 276 |
| <b>Table 10.</b> | MS data of EDOT-OCO-H3H3. ....  | 277 |
| <b>Table 11.</b> | <sup>1</sup> H NMR data of EDOT-OCO-H1H2 in CDCl <sub>3</sub> .....   | 278 |
| <b>Table 12.</b> | <sup>13</sup> C NMR data of EDOT-OCO-H1H2 in CDCl <sub>3</sub> . .... | 279 |
| <b>Table 13.</b> | MS data of EDOT-OCO-H1H2.....   | 280 |
| <b>Table 14.</b> | <sup>1</sup> H NMR data of EDOT-OCO-H1H3 in CDCl <sub>3</sub> .....   | 281 |
| <b>Table 15.</b> | <sup>13</sup> C NMR data of EDOT-OCO-H1H3 in CDCl <sub>3</sub> . .... | 282 |
| <b>Table 16.</b> | MS data of EDOT-OCO-H1H3.....   | 283 |
| <b>Table 17.</b> | <sup>1</sup> H NMR data of EDOT-OCO-H1H4 in CDCl <sub>3</sub> .....   | 284 |
| <b>Table 18.</b> | <sup>13</sup> C NMR data of EDOT-OCO-H1H4 in CDCl <sub>3</sub> . .... | 285 |
| <b>Table 19.</b> | MS data of EDOT-OCO-H1H4.....   | 286 |
| <b>Table 20.</b> | <sup>1</sup> H NMR data of EDOT-OCO-H1H5 in CDCl <sub>3</sub> .....   | 287 |
| <b>Table 21.</b> | <sup>13</sup> C NMR data of EDOT-OCO-H1H5 in CDCl <sub>3</sub> . .... | 288 |
| <b>Table 22.</b> | MS data of EDOT-OCO-H1H5.....   | 289 |



## Glossary

|   |   |
|---|---|
| AAO   | Anodic Aluminum Oxide   |
| AFM   | Atomic Force Microscopy   |
| Bu <sub>4</sub> NBF <sub>4</sub>                                | Tetrabutylammonium tetrafluoroborate  |
| Bu <sub>4</sub> NC <sub>4</sub> F <sub>9</sub> SO <sub>3</sub>  | Tetrabutylammonium nonafluorobutanesulfonate                                  |
| Bu <sub>4</sub> NC <sub>8</sub> F <sub>17</sub> SO <sub>3</sub> | Tetrabutylammonium heptadecafluorooctanesulfonate                             |
| Bu <sub>4</sub> NCF <sub>3</sub> SO <sub>3</sub>                | Tetrabutylammonium trifluoromethanesulfonate                                  |
| Bu <sub>4</sub> NCIO <sub>4</sub>                               | Tetrabutylammonium perchlorate  |
| Bu <sub>4</sub> NPF <sub>6</sub>                                | Tetrabutylammonium Hexafluorophosphate  |
| CV  | Cyclic Voltammetry  |
| d   | Doublet   |
| dd  | Doublet of doublet  |
| DMAP  | 4-(dimethylamino)pyridine   |
| DMF   | Dimethylformamide   |
| E <sub>1/2</sub>  | Half-wave potential   |
| ECA   | ethyl-cyanoacrylate   |
| EDC   | <i>N</i> -(3-dimethylaminopropyl)- <i>N</i> '-ethylcarbodiimide hydrochloride |
| EDOT  | 3,4-Ethylenedioxythiophene  |
| EOTT  | 3,4-Ethyleneoxythiathiophene  |
| EOTT  | 3,4-ethyleneoxythiathiophene  |
| E <sup>ox</sup>   | Monomer oxidation potential   |
| E <sub>ox, polym</sub>  | Polymer oxidation potential   |
| E <sub>ox</sub>   | Monomer oxidation potential   |

|                         |   |
|-------------------------|---|
| $E_{\text{ox,opt}}$     | Optimal oxidation potential                       |
| $E_{\text{red, polym}}$ | Polymer Reduction Potential                       |
| GC-MS                   | Gas Chromatography coupled with Mass Spectroscopy |
| $H_{\text{liquid}}$     | Hysteresis measured with liquid droplet           |
| HDPE                    | High Density Poly(ethylene)                       |
| HFDT                    | Heptadecafluoro-1-decanethiol                     |
| J                       | Coupling Constant                                 |
| LbL                     | Layer-by-Layer                                    |
| LDPE                    | Low Density Poly(ethylene)                        |
| m                       | Multiplet   |
| m.p.                    | Melting point                                     |
| $\text{NaClO}_4$        | Sodium perchlorate                                |
| NMR                     | Nuclear Magnetic Resonance                        |
| PAA                     | Poly(acrylic acid)                                |
| PAN                     | Polyacrylonitrile                                 |
| PANI                    | Polyaniline                                       |
| PC                      | Polycarbonate                                     |
| PCL                     | Polycaprolactone                                  |
| PDMS                    | Poly(dimethylsiloxane)                            |
| PE                      | Polyethylene                                      |
| PECA                    | Poly(ethyl-cyanoacrylate)                         |
| PEDOT                   | poly(3,4-ethylenedioxythiophene)                  |
| PEDOT                   | Poly(3,4-ethylenedioxythiophene)                  |
| PEI                     | Poly(ethyleneimine)                               |
| PEOT                    | poly(3,4-ethyleneoxythiathiophene)                |
| PET                     | Polyethylene terephthalate                        |

---

|                  |  |
|------------------|--|
| PFDA             | Poly(heptadecafluorodecylacrylate)                       |
| PFO <sup>-</sup> | Perfluorooctanoate anion                                 |
| PFTDS            | <i>1H,1H,2H,2H</i> -perfluorodecyltrichlorosilane        |
| PHFMA            | Poly(2,2,3,4,4,4-hexafluorobutyl methacrylate)           |
| PMETAC           | Poly[2-(methacryloyloxy)ethyltrimethylammonium chloride] |
| PMMA             | Poly(methyl methacrylate)                                |
| PNIPAAm          | Poly(N-isopropylacrylamide)                              |
| POSS             | Polyhedral oligomeric silsesquioxane                     |
| PP               | Poly(propylene)  |
| PProDOT          | Poly(3,4-propylenedioxythiophene)                        |
| PProDOP          | Poly(3,4-propylenedioxy pyrrole)                         |
| PS               | Poly(styrene)  |
| Pt               | Platinum   |
| PTFE             | Poly(tetrafluoroethylene)                                |
| pTSA             | <i>p</i> -toluenesulfonic acid                           |
| PU               | Polyurethane   |
| PUA              | Polyurethane acrylate                                    |
| PVC              | Poly(vinyl chloride)                                     |
| PVDF             | Poly(vinylidene fluoride)                                |
| PVDMA            | Poly(2-vinyl-4,4-dimethylazlactone)                      |
| Qs               | Deposition charge  |
| r                | Wenzel Roughness factor                                  |
| r.t.             | Retention time   |
| R <sub>a</sub>   | Arithmetic Roughness                                     |
| R <sub>q</sub>   | Root Mean Square Roughness                               |
| s                | Singlet  |

|                          |   |
|--------------------------|---|
| SCE                      | Saturated Calomel Electrode                                 |
| SEM                      | Scanning Electron Microscopy                                |
| sept.                    | Septuplet   |
| sext.                    | Sextuplet   |
| SI-ATRP                  | Surface-Initiated Atom Transfer Radical Polymerization      |
| t                        | Triplet   |
| TEOS                     | Tetraethyl orthosilicate                                    |
| THF                      | Tetrahydrofuran   |
| tt                       | Triplet of triplet  |
| UV                       | Ultra-violet  |
| $\alpha_{\text{liquid}}$ | Sliding angle measured for liquid                           |
| $\gamma_{\text{LV}}$     | Interfacial tension between Liquid-Vapor                    |
| $\gamma_{\text{SL}}$     | Interfacial tension between Solid-Liquid                    |
| $\gamma_{\text{SV}}$     | Interfacial tension between Solid-Vapor                     |
| $\delta$                 | Chemical shift  |
| $\theta_a$               | Advancing angle   |
| $\theta^{\text{CB}}$     | Apparent contact angle determined by Cassie-Baxter equation |
| $\theta_{\text{diiodo}}$ | Static diiodomethane contact angle                          |
| $\theta_r$               | Receding angle  |
| $\theta^{\text{W}}$      | Apparent contact angle determined by Wenzel equation        |
| $\theta_{\text{water}}$  | Static water contact angle                                  |
| $\theta_{\text{water}}$  | Water contact angle   |
| $\theta^{\text{Y}}$      | Contact angle of Young's equation                           |
| $\phi_a$                 | Air Fraction  |
| $\phi_s$                 | Solid fraction  |



# Introduction

From a chemist's point of view, making an hydrophobic surface is possible by using an hydrophobic bulk or by making surface modifications such as coating the surface with a polymer, activating and grafting hydrophobic molecules onto the surface, making self-assembled monolayers onto the surface or depositing self-assembled monolayers or hyperbranched polymers for example (Figure 1). With all these techniques, hydrophobic surfaces are mainly flat.

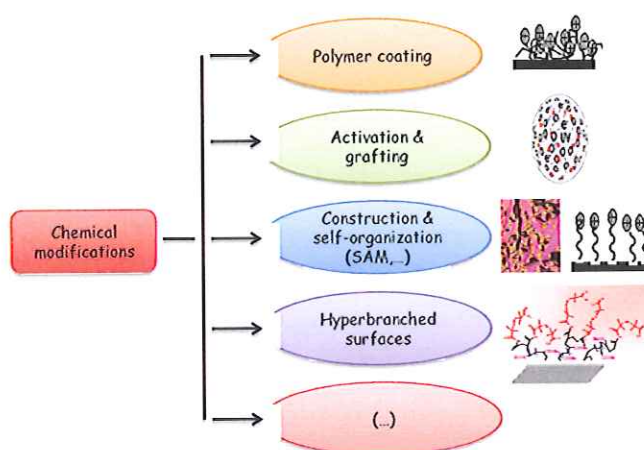


**Figure 1.** Examples of chemical modifications to produce hydrophobic surfaces.

The hydrophobicity comes from the intrinsic hydrophobicity of the bulk or the deposited species. The water-repellency is evaluated by measuring the contact

angle between the water droplet's tangent and the solid surface's tangent. With these techniques described in Figure 1, the highest water contact angle we could obtain was  $120^\circ$  which corresponds to the smooth surface of poly(tetrafluoroethylene) (PTFE). In 2000, Genzer and his co-workers previously stretched their surface before grafting a self-assembled monolayer of fluorinated compounds (Genzer, J; Efimenko, K. *Science* **2000**, *290*, 2130-2133). From this technique, they deposited a mechanically assembled monolayer (MAM) instead of a self-assembled monolayer (SAM). Thus, they enhanced the density of the grafted molecules and they increased the water-repellency with a water contact angle of  $130$ - $135^\circ$ .

Fluorinated compounds are often employed to fabricate hydrophobic surface. The advantages are their chemical and thermal inertia as well as their low surface energy. However due to their chemical inertia, long fluorinated tails are not easily degradable. As a consequence, it is very difficult or quasi impossible for the body of living species to eliminate these compounds. Long fluorinated tails are thus considered as bioaccumulable species. In opposition to synthetic pathway proposed in literature, in nature, we can find surfaces with extreme water-repellency properties (i.e. on which water droplets remained spherical) without

using fluorine chemistry. These surfaces are named superhydrophobic. This phenomenon could be explained by an appropriate combination of either morphology, either roughness or surface structuration and low surface energy raw materials. Hence, the main subject of this research work was to find alternative to fluorine chemistry by the preparation of superhydrophobic material within hydrocarbon series.

In literature, several techniques to produce superhydrophobic surfaces have been described. Amongst them, electrochemical polymerization allowed the design of surfaces with special wettability and especially the possibility to obtain superhydrophobic surfaces. The main advantages of this technique are:

- The speed: the deposition and the surface structuration occur at the same time
- The versatility: an accurate design of the monomer chemical structure influences the resultant morphology and properties. it is also possible to control the morphology through the electrochemical parameters (deposition charge, supporting electrolyte, solvent, deposition technique, etc)

In this thesis, the challenges were:

1. To make an assessment of the existed techniques to produce superhydrophobic surfaces with polymer material
2. To focus on superhydrophobic fibrous polymers since fibers present many practical applications
3. To produce superhydrophobic surfaces with hydrocarbon conducting polymers
4. To evaluate the influence of chemical and physical part onto the wetting properties
5. To compare hydrocarbon conducting polymers with fluorinated analogues
6. To study the impact of the polymerizable core onto the properties.

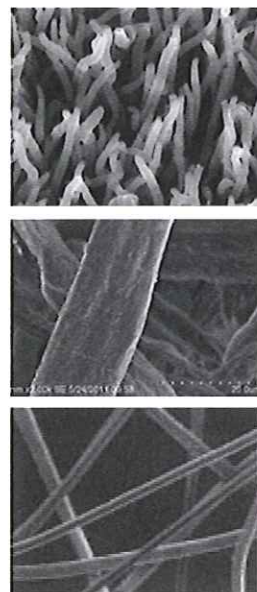
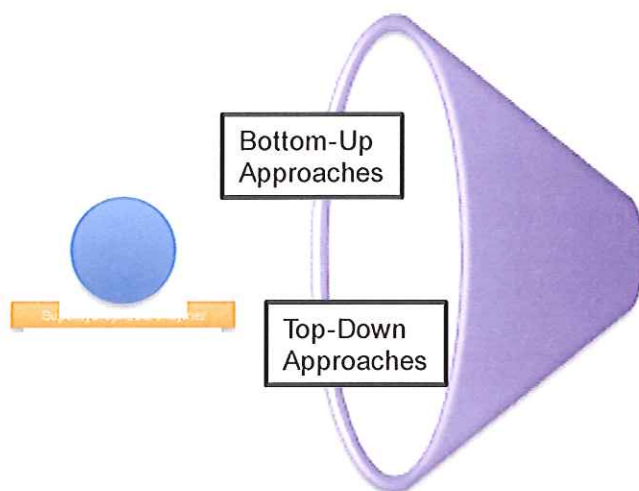
All these challenges can be summed up in Figure 2.

This work is thus divided into four chapters. First, we will present a review of the techniques employed to obtain superhydrophobic polymers then superhydrophobic fibrous polymer surfaces. The second chapter is devoted to one particular hydrocarbon ethylenedioxythiophene (EDOT) series. We will see if superhydrophobicity could be reached with these polymers and if we can get chemical and physical parts impacting onto the wetting properties. Finally, the fourth chapter will describe the surfaces properties comparison between



hydrocarbon and fluorinated surfaces as well as the influence of polymerizable core onto the resultant surface properties.

Chap. 1

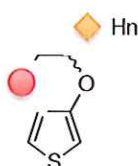


Chap. 2



- Superhydrophobicity with Hydrocarbon conducting polymers?
- % of Chemistry and Physics onto Contact angle?

Chap. 3



- Hn vs. Fn
- Influence of Polymerizable core?

Figure 2. Thesis synoptic representation.